ОБЪЕДИНЕННЫЙ
ИНСТИТУТ
ЯДЕРНЫХ
ИССЛЕДОВАНИЙ

Дубна

E15-2000-256

J.Adam[1], A.Balabekyan[2], R.Brandt[3], V.P.Dzhelepov, S.A.Gustov, V.G.Kalinnikov, M.I.Krivopustov, I.V.Mirokhin, J.Mrazek[1], R.Odoj[4], V.S.Pronskikh, O.V.Savchenko, A.N.Sosnin, A.A.Solnyshkin, V.I.Stegailov, V.M.Tsoupko-Sitnikov

INVESTIGATION OF THE FORMATION OF RESIDUAL NUCLEI FROM THE RADIOACTIVE ^{237}Np AND ^{241}Am TARGETS IN THE REACTION WITH 660 MeV PROTONS

Submitted to «Ядерная физика»

[1]Institute of Nuclear Physics, Řež, Czech Republic
[2]Yerevan State University, Armenia
[3]Institut für Physikalische, Kern- and Makromolekular Chemie, Philipps-Universität, Marburg, Germany
[4]Forschungszentrum Jülich, Germany

2000

The present work was initiated by the prominent scientist and outstanding man V.P.Dzhelepov. The preliminary results were reported by him at the JINR Scientific Council. This investigation is one of the last initiated by V.P.Dzhelepov with great enthusiasm , but his untimely death prevented him from seeing the final results. The death of V.P.Dzhelepov is an irreparable loss for Russian Science and for all those who knew him and worked with him.

Introduction

The transmutation of fission products and actinoids produced in atomic power stations has aroused great interest in the last decade. Estimations made by different groups [1,2] point out that in the case of transmutation of all transuranium elements (TUE) radiation risk due to their leakage from the deep underground storage systems must be compared with the natural radioactivity of the uranium ore after 10^3 years and not after $5 \cdot 10^6$ years (as in the case of untreated wastes). But in this case treatment of TUE at all stages of the fuel cycle becomes a more difficult problem.

Estimations of radiation risk of the spent nuclear fuel (SNF) show that after extraction of the uran-plutonium actinoid group and such fission products as ^{90}Sr and ^{137}Cs the main risk for the population can be associated with ^{241}Am and ^{237}Np [3]. Among actinoids ^{241}Am makes the greatest contribution. The particular hazardous effect of ^{237}Np is due to its mass predominance and high migration ability, which increases the probability of its penetration in a human body through the food chaines [4].

The investigation of ^{237}Np and ^{241}Am transmutation dynamic in the flow of thermal neutrons of different densities shows that the higher the density of neutrons, the smaller the number of different actinoids noticeably contributing to radioactivity of wastes [4]. For solving the problem of the transmutation High-current proton accelerators must be used to produce neutron fluxes of 10^{17} $cm^{-2}c^{-1}$ for transmutation purposes. In some recent publications both transmutation of actinoids under the effect of neutron irradiation and their spallation and fission under the effect of proton and ion beams are investigated [5].

Parameters of the hadron-nucleon cascade are the basis for calculations of electronuclear setups, their targets and the blanket effect. These parameters are calculated with a number of codes using models of different accuracy for the cascade approximation. As is shown in [6] the best test for different codes is comparison of calculated and experimental yields of residual nuclei. From the experimental point of view, determination of the independent cross-section for yields of short-lived nuclear products from the monoisotope target is most important for the comparison [7]. Experimental cross-sections for residual nuclei in radioactive ^{241}Am and ^{237}Np targets are imdoubtedly important for the projects of transuranium waste transmutation in a direct proton beam [8]. The present paper deals with the investigation of the cross-sections for formation of residual nuclei in ^{241}Am and ^{237}Np targets.

Experimental method

The experiment was carried out on the external beam of the JINR LNP Phasotron with a beam current of 1.2 μA. The NpO_2(Np) and AmO_2(Am) targets were exposed to the proton beam with the energy of 660 MeV. The target and beam characteristics are presented in Table 1.

Table 1. Characteristics of the $^{237}_{93}Np$ and $^{241}_{95}Am$ targets.

Target	$^{237}_{93}Np$		$^{241}_{95}Am$	
Half life [years]	$2.144(7)10^6$		432.2(7)	
Total mass attenuation coefficient for γ-rays with energy of 300 keV[cm^2/g]	0.498		0.508	
Density of oxide [g/cm^3]	11.1		11.7	
Weight[g]	0.742	0.742	0.177	0.183
Thickness[mm]	0.193	0.193	0.043	0.044
Activity [mCi]	0.523	0.523	601	621
Beam intensity [10^{14}p/min]	2.64	2.66	2.72	2.58
Irradiation times [min]	5	30	5	30

The irradiated target samples were hermetically packed in aluminium capsules with a weight of 78.8 g, and dimensions shown in Figure 1.

Figure 1. The $^{237}_{93}Np$ and $^{241}_{95}Am$ targets in an aluminium capsule.

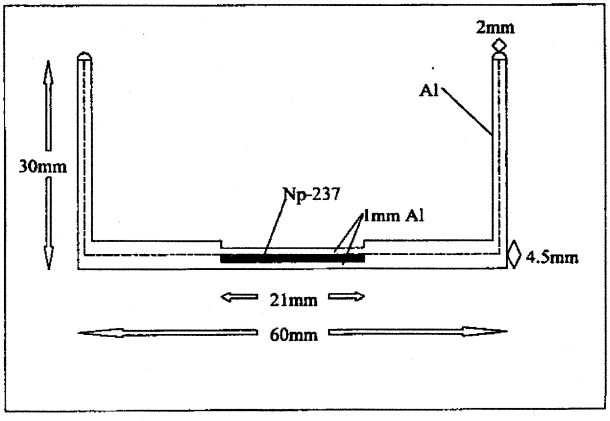

new values of the reaction cross-section at the energy higher than 800MeV, but in our energy range it value did not change [12]. In our calculation we used the cross-section of the reaction $^{27}Al(p,3pn)\,^{24}Na$ represented above. Aluminium foils of the same dimensions as the targets were used for monitoring. The weight of each aluminium foil was 99mg. The targets were irradiated in two steps: 5-minute exposure for measurement of short-lived residual nuclides and 30-minute exposure for long-lived ones.

The induced activity of the targets was measured by two detectors, an HPGe detector with the 20 % efficiency and an energy resolution of 1.8 KeV (1332 KeV ^{60}Co) for the ^{241}Am target and a Ge(Li) detector with the 4.8 % efficiency and a resolution of 2.6 keV (1332 keV ^{60}Co) for the ^{237}Np target. Recording of the γ spectrum was carried out with a high-rate multichannel buffer MASTER 921 (^{241}Am) and a 4-input multichannel buffer MASTER 919 (^{237}Np), which automaticaly determined the dead time.

The measurement of the first targets (short exposures) started 10 minute after the end of the irradiation. These targets were measured 17 times during 17 hours. The measurement time varied from 5 minutes to 3 hours, the distances between the target and the detector were 150 cm for ^{241}Am and 100 cm for ^{237}Np. The second targets (30-minute exposures) were measured 11 times during 30 days with exposures from 5 to 50 hours and respective distances 100 and 60 cm. The code DEIMOS [13] was used in interactive mode for spectrum handling. This code determines the area S_γ and the position K_γ of the peak and the upper limit of the peak area $S_\gamma(lim)$, which cannot be found at the given background level. At the same time the exact energy E_γ and intensity I_γ of the peaks can be obtained. When the spectrum handling was finished, the data were "cleaned" from background lines, single and double escape peaks. Peak intensities were corrected by subtraction of the piled-up single and double escape peaks. The corrected line intensities were used for determing the half-life of every line, including the complex (doublet) lines. Identification of the residual nuclei was based on their γ transition energies and intensities and half lives compared with the data from the Atomic Data and Nuclear Data Tables [14]. More detailed analysis and checking of the data after identification of residual nuclei for the ^{241}Am target were made with a special code. This analysis is based on comparison of the ratios between our experimental $I_\gamma(lim)$ (<--S_γ (lim)) and published I_γ (lit) intensities of the transitions (including unobserved ones) for each decaying identified nucleus. Knowing the half-lives of the multiplet components we also analysed such complex lines. We found 1025 γ-lines in 28 spectra measured for ^{241}Am targets; 166 of them had different energies E_γ. Determining half-lives of those 166 lines, we found that 34 of them are doublets and 5 are triplets. A special system of codes was created for complex analysis of the experimental data. This system is described in detail in [15].

The cross-sections of formation of residual nuclei (*a*) $\sigma_a(E_\gamma(j))$ were determined for each line in all the measured spectra i=1,2,...n with correction for the dead time (equation 2, Table 2)

$$\sigma_a(E_\gamma(j),i)=\frac{S_i(E_\gamma(j))\lambda_a \dfrac{t_3(real,i)}{t_3(live,i)}}{N_p N_{t\,\mathrm{arg}} \varepsilon_\gamma(E_\gamma(j)) I(E_\gamma(j))(1-e^{-\lambda_a t_1(i)})e^{-\lambda_a t_2(i)}(1-e^{-\lambda_a t_3(real,i)})}\,, \qquad (2)$$

were $S_i(E_\gamma(j))$ is the number of recorded γ-quanta with the energy $E_\gamma(j)$ in the ith spectrum; λ_a [s^{-1}] is the decay constant of nucleus a; N_p is the flux of particles [s^{-1}] on the target; N_{targ} is the number of nuclei on 1 cm^2 of the target surface; $\varepsilon_\gamma(E_\gamma(j))$ is the absolute recording efficiency for γ-quanta with the energy $E_\gamma(j)$; $I_\gamma(E_\gamma(j))$ is the intensity per

decay of γ-rays with the energy $E_\gamma(j)$; t_1, $t_2(i)$, $t_3(real,i)$, $t_3(live,i)$ - the exposure time waiting time, real and live time of measurement respectively.

The components of the doublet lines are genetically related (decay of the mother nucleus a and of the daughter nucleus b) or independent (nuclei a', b'). The number of γ-rays from the decay of nucleus b recorded in the ith measurement is

$$S_i\left(E_{\gamma(b)}\right)=\left\{Ae^{-\lambda_a t_2(i)}\left(1-e^{-\lambda_a t_3(real,i)}\right)+Be^{-\lambda_b t_2(i)}\left(1-e^{-\lambda_a t_3(real,i)}\right)\right\}\frac{t_3(live,i)}{t_3(real,i)} \qquad (3)$$

Substituting the known λ_a , λ_b and measured values $S_i(E_\gamma(b))$, $t_2(i)$, $t_3(real,i)$ and t_3 (live,i), we calculate the coefficients A and B by the least squares method from several measurement i=1,2,... and determine the cross-sections for genetically related residual nuclei:

$$\sigma_a=\frac{\lambda_a\left(\lambda_b-\lambda_a\right)}{K_b\lambda_b\left(1-e^{-\lambda_a t_1}\right)}\times A \qquad (4)$$

$$\sigma_b=\frac{\lambda_b}{K_b\left(1-e^{-\lambda_b t_1}\right)}\times B+\frac{\lambda_a^{\,2}}{K_b\lambda_b\left(1-e^{-\lambda_a t_1}\right)}\times A\ , \qquad (5)$$

where

$$K_b=N_p N_{t\,\mathrm{arg}}\varepsilon_\gamma^{abs}\left(E_\gamma\right)I_\gamma\left(E_\gamma,b\right) \qquad (6)$$

If we replace the coefficient A by A' and B by B', equation (2) will be valid for the independent decay of nuclei a',b'. Then the cross-sections of formation of the residual nuclei can be found from the relations:

$$\sigma_a=\frac{\lambda_a}{K_b\left(1-e^{-\lambda_a t_1}\right)}\times A' \qquad (7)$$

$$\sigma_b=\frac{\lambda_b}{K_b\left(1-e^{-\lambda_b t_1}\right)}\times B' \qquad (8)$$

We also obtained a similar equation for the triplet lines. The results of the analysis of the multiplet peaks are presented in Table 3. In some cases we performed the fixed value fitting of one of these cross-sections (σ_a, σ_b ,or σ_c). Small values of χ^2 prove correctness of the analysis of complex lines for residual nuclei.

About ~60 residual nuclei from the ^{237}Np target and 80 residual nuclei from the ^{241}Am target were found. The results are demonstrated in Tables 4 and 5. The errors in the tables are the largest deviation of the given cross-section from the average-weighted cross-section of several measurements.

Experimental results and discussions

The cross-sections of formation of nuclei from the ^{231}Np and ^{241}Am targets are shown in Tables 4 and 5. The final results for the ^{241}Am target are presented in Table 5. For 44 nuclei the cross-section were determined from several γ-transitions: in 33 cases the weighted average

value was found from two γ-transitions, in 7 cases from three, in one case from four and in three cases from six γ-transitions (Table 2). Gamma transitions, assigned to the decay of the residual nuclei ^{7}Be, ^{22}Na, ^{24}Na, ^{27}Mg and ^{28}Al were detected. The first three nuclei could be formed in the reactions p+^{241}Am and p+^{27}Al (targets packed in the aluminium capsule). If we assume that they appear in the Al capsule, we obtain the following cross-sections for their formation σ(^{7}Be)= (5.5±0.5)mb, σ(^{22}Na)= (16.4±1.4)mb and σ (^{24}Na)= (12.3±1.1)mb. These values agree within the error with the literature values of cross-sections of formation of the ^{7}Be, ^{22}Na, ^{24}Na nuclei on the Al target exposed 660 MeV protons [16]: σ(^{7}Be)= 5.0mb, σ(^{22}Na)= 15.0mb and σ(^{24}Na)=10.8mb. The residual nuclei ^{27}Mg and ^{28}Al could be produced in the reactions (n,p) and (n,γ) from the ^{27}Al target. Using the literature values for these reactions σ(Al(n,p)^{27}Mg)=52.5mb [17] and σ(Al(n, γ)^{28}Al)=(230±5)mb [18] we can estimate the flux of the secondary and background neutrons in which the aluminium capsule finds itself (fig.1). It is $4\cdot10^{12}$ n/min (E_n>4.5MeV) from the first reaction, and $2\cdot10^{11}$ n/min from the second one.

The tables show not only the type of the cross-sections of the formation of the given residual nucleus (I--independent cross-section, C - cumulative cross-section), but also the decay mode of this nucleus (β^--β^+- decay or electron capture). For comparison, the theoretical cross-section calculated by cascade-evaporation model are also presented [19].

The theoretical calculation were based on simulation of 1000000 events. Since the calculation yields only independent cross-sections of the residual nuclei a correction was made for them then the experimental cumulative cross-sections to make comparison valid. The isobar chain (A = const) of β-decaying n and m residual nuclei together with their isomers (one nucleus is able to form more than one isomers) can be presented as follows:

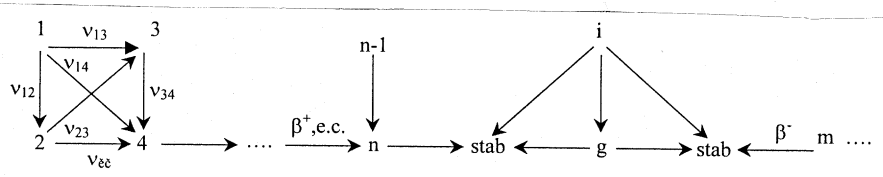

where the odd numbers denote formation of isomeric states of the residual nuclei whose ground states are denoted by the even numbers. $\nu_{k,k+1}$, $\nu_{k,k+2}$, $\nu_{k,k+3}$ are the branching coefficients of the decay of the isomeric state (k is odd) and $\nu_{1,1+1}$, $\nu_{1,1+2}$ (l is even) are the branching coefficients of the decay of the ground states. The cumulative yield of the nth residual nucleus is calculated by the generalized formula that followes from the physical interpretation of the independent and cumulative yields:

$$\sigma_n^{cum} = \sigma_n^{ind} + \sum_{m=1}^{n-1} B_{mn}\sigma_m^{ind} \qquad (9)$$

$$B_{mn} = \nu_{mn} + \sum_{l_1>m}^{n-1} \nu_{ml_1}\nu_{l_1n} + \sum_{l_2>l_1}^{n-1}\sum_{l_1>m}^{n-2} \nu_{ml_1}\nu_{l_1l_2}\nu_{l_2n} + \ldots$$

$\nu_{mn} \equiv 0$ if n-m>3 for odd m, or if n-m>2, for even m. For even isobars there exists a nucleus g (and its isomer i) near the stability line, that disintegrates through β^- decay, β^+ decay and electron capture. Formation of such nuclei is characterized by independent cross-sections. Tables 4, 5 demonstrate the theoretical cross-sections for the ground states of the residual

nuclei. The calculation accuracy parameter (deviation factor) could be the mean ratio of the calculated $\sigma_{calc}(i)$ to the experimental $\sigma_{exp}(i)$

$$\langle H \rangle = 10^{\sqrt{\langle [\log[\sigma_{calc}(i)/\sigma_{exp}(i)]]^2 \rangle}} \tag{10}$$

with the standard deviation $S(<H>) = 10^{\sqrt{a}}$, where

$$a = < \left[\left| \log\left(\frac{\sigma_{calc}(i)}{\sigma_{exp}(i)} \right) \right| - \log(< H >) \right]^2 > \tag{11}$$

On the basis of the data in Tables 4, 5 we obtaine:

	^{237}Np	^{241}Am
<H>	9.68	5.5
S(<H>)	4.68	3.7

Figures 3 and 4 show the cross-sections of the formation of the residual nuclei as a function of their mass number. The residual nuclei are seen to be fission products [20]. However, the nuclei with A>160, i.e. with the mass number close to the target were formed only by spallation. As seen from Tables 4 and 5 and from figures residual nuclei with the half-life from several minutes to several months dominate. They decay to stable isotope. The cross-sections for some residual nuclei -- ^{95}Tc, ^{106m}Ag, ^{110m}Ag, ^{118m}Sb are small that is why they became an exception from the basic dependence. This is due to the fact that only isomer states of these residual nuclei were recorded. In [21] it was shown that for proton-nuclear reactions in a target of tin isotopes the isomeric ratio of the cross-section for high-spin state formation to that for-low spin state depends on the number of the emitted neutrons and can be as large as 6-7. For example, for the nucleus ^{95}Tc it is $\sigma(^{95g}Tc(9/2^+))/\sigma(^{95m}Tc(1/2^-)) \sim 7$. Therefore, we can conclude that the cross-sections of the isomeric nuclei dropping out of the basic dependence (Fig. 3,4) can be increased by the cross-section for the ground state and then these points could fall on the curve too. Analysing types of formation of the residual nuclei we can see that the experimental numbers of the neutron-rich nuclei and neutron-deficient nuclei are equal. Our results were compared with the results of [5]. The comparison shows that because of the great intensity of our beam (three orders of magnitude higher ($1.3 \cdot 10^{16}$p/hour), the number of residual nuclei is larger than in [5].

The authors are grateful to the personnel of the phasotron for providing good parameters of the beams. The authors thanks also the Directorate of the Laboratory of High Energies of JINR for providing us with radioactive targets.

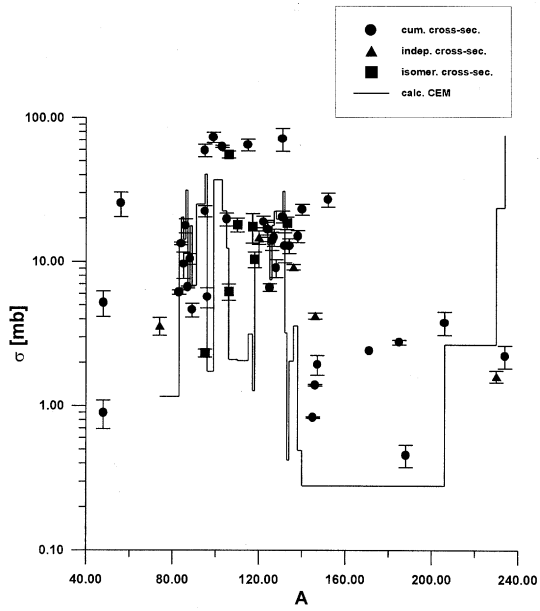

Figure 3. Dependence of cross-sections of formation of residual nuclei on the mass number of these nuclei for the ^{237}Np target.

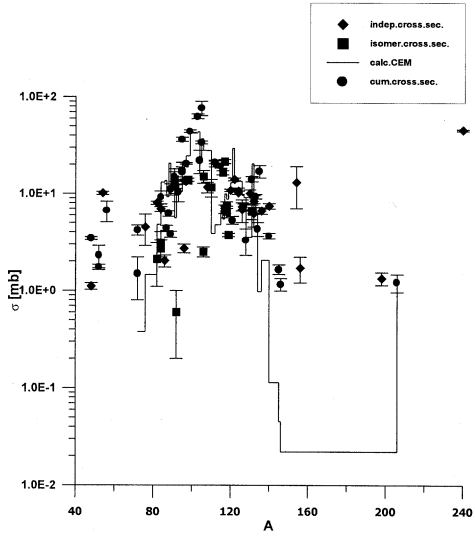

Fig.4 Dependence of cross-sections of formation of residual nuclei on their mass number for the ^{241}Am target.

Table 2. Residual nuclei from the reactions $^{241}Am(p,xpyn)X$

Resid.nucl.	$T_{1/2}$	E_γ	I_γ	Cross-sec.[mb]	Amount of measurem.
^{48}Sc	1.820(4)d	c983.500(1)	1.0	1.35±0.19	7
		c1312.100(30)	0.975	1.04±0.10	7
^{48}V	15.970(10)d	C983.50(3)	0.9999	3.52±0.17	7
		c1312.00(3)	0.9739(20)	3.37±0.14	7
^{52}V	3.750(10)m	1434.100(10)	1.000(10)	2.3±0.6	1
^{52}Mn	5.590(10)d	c744.233(13)	0.906(4)	1.81±0.20	1
		c935.544(12)	0.949(3)	1.9±3.4	4
		1434.090(17)	1.000(3)	1.71±0.12	1
^{54}Mn	312.5(5)d	c834.830(21)	0.9998(2)	10.1±0.4	9
^{56}Mn	2.580(1)h	846.750(20)	0.9887(30)	6.7±1.6	7
^{72}Ga	14.100(11)h	c834.030(30)	0.9563	1.5±0.7	9
^{72}As	1.080(5)d	c833.990(30)	0.795	4.2±0.5	8
^{76}As	1.1000(30)d	c559.10(5)	0.447(8)	4.5±1.6	5
^{76}Br	16.19(22)h	c559.09(5)	0.740	0.6±1.9	5
^{82}Br	1.470(20)d	c554.320(20)	0.706(4)	7.55±0.30	5
		c619.070(20)	0.431(5)	10.5±0.9	10
		c698.330(20)	0.279(4)	8.5±0.9	2
		c776.490(30)	0.834	8.68±0.30	7
		c827.810(30)	0.2419(25)	7.3±0.6	5
		c1043.970(30)	0.2736(33)	6.5±0.6	5
		c1317.47(5)	0.2694(33)	8.0±0.4	5
		1474.82(8)	0.1660(17)	8.6±0.7	2
^{84}Br	6.470(6)h	c554.35(10)	0.624(8)	12±5	5
		c619.11(10)	0.380	6±7	10
		c698.37(10)	0.263(7)	2.5±0.8fix	2
		c776.52(10)	0.844	1.4±1.7	7
		c827.83(10)	0.210(6)	7±11	5
		c1044.08(10)	0.321	2.5±0.4fix	5
		c1317.43(10)	0.237(6)	10±12	5
^{84}Rb	32.77(14)d	c881.610(3)	0.690(20)	6.9±0.4	5
^{86}Rb	18.82(2)d	1076.6(1)	0.0878	2.02±0.30	1
^{89}Rb	15.15(14)m	c657.77(6)	0.0998(52)	4±8	4
		c947.73(7)	0.0922(46)	23±6	1
		1031.92(6)	0.58(3)	10.6±0.8	4
		1248.14(6)	0.423(23)	10.7±1.4	3
		2195.92(11)	0.1334(87)	23±5	1
^{91}Sr	9.52(6)h	c555.60(10)	0.617(6)	0.9±7.0	17
		c1024.30(10)	0.334	15.0±1.8	10
^{92}Sr	2.710(10)h	1383.90(6)	0.9(1)	11.8±0.5	12
^{93}Sr	7.32(10)m	590.28(5)	0.665(18)	13.4±2.7	3

		875.73(6)	0.239(13)	7.1±2.8	1
^{84m}Y	40(1)m	793.0(3)	0.986	3.1±0.9	1
^{87}Y	3.350(10)d	484.90(5)	0.922(10)	4.40±0.29	6
^{88}Y	106.6(4)d	898.021(19)	0.940(4)	6.5±0.6	3
		1836.01(4)	0.9936(2)	6.1±0.5	3
^{91m}Y	49.71(4)m	555.57(10)	0.949(6)	14±4	17
^{95}Y	10.30(10)m	954.20(20)	0.19	18±4	1
^{89}Zr	3.270(10)d	909.20(10)	0.9987	3.79±0.29	1
^{95}Zr	63.98(6)d	c724.23(4)	0.4444(60)	36.0±2.0	4
		756.74(4)	0.5486	38±4	5
^{97}Zr	16.90(5)h	cd657.92(10)	0.9135(11)	20.7±0.4	8
		cd743.36(10)	0.9093(6)	19.5±0.8	3
^{92m}Nb	10.15(2)d	c935.44(10)	0.99	0.6±0.4	4
^{95}Nb	33.15(5)d	c765.83(4)	1.0	16.8±2.1	8
^{96}Nb	23.35(5)h	460.03(6)	0.276(11)	15±2.0	3
		568.86(6)	0.546(22)	12.5±0.6	8
		c719.56(15)	0.0713(4)	35±18	4
		c778.22(10)	0.950	13±2	10
		810.25(7)	0.0969(61)	15±4	8
		c849.90(10)	0.203(10)	13.2±1.7	10
		1091.31(6)	0.484(22)	13.8±0.4	7
		1200.19(6)	0.197(10)	14.7±0.9	4
^{97}Nb	1.200(12)h	c657.92(10)	0.9834(11)	13.3±0.8	17
^{98m}Nb	51.30(40)min	c722.50(10)	0.707(65)	12.2±0.7	17
		787.20(10)	0.93(8)	15±0.7	9
^{99}Mo	2.750(8)d	c739.500(15)	0.1219	44.1±1.3	10
^{96}Tc	4.30(10)d	c778.22(4)	0.9976	2.71±0.29	10
		812.54(4)	0.820(35)	2.65±0.14	6
		c849.86(4)	0.976(38)	2.78±0.19	10
^{104}Tc	18.4(10)min	358.00(10)	0.89	28±8	1
		c884.40(10)	0.110(12)	14±8	1
^{103}Ru	39.35(5)d	497.080(13)	0.889(28)	63±4	8
^{105}Ru	40440(22)h	676.36(8)	0.157(5)	40±4	6
		c724.30(3)	0.473	33.0±1.3	15
^{105}Rh	1.470(1)d	318.90(10)	0.192	77±13	2
^{106m}Rh	2.170(34)h	717.20(10)	0.294(34)	13.8±2.5	2
		748.50(10)	0.197(23)	21±5	1
		1529.40(10)	0.178(24)	17±4	1
^{108}Rh	5.90(20)min	581.10(20)	0.586	9.5±1.9	1
		c947.10(20)	0.4974	13.9±1.9	1
^{112}Pd	21.05(5)h	cd617.40(20)	0.43(60)	18±3	9
		cd694.80(20)	0.0345(8)	41±9+e	8
^{106m}Ag	8.46(10)d	c1045.83(8)	0.2955(96)	2.4±0.4	5
		1527.65(19)	0.163(13)	2.6±0.5	1

^{110m}Ag	252.2(3)d	c657.70(10) 884.70(10)	0.947 0.729	21±11 11.2±2.6	8 3
^{112}Ag	3.140(20)h	617.40(20)	0.43(6)	20.4±1.7	13
^{115}Cd	2.230(4)d	492.350(4) 527.900(7)	0.0803(33) 0.274(11)	18±4 19.3±0.9	1 7
^{117m}Cd	3.36(5)h	c552.900(20)	0.997(10)	6.9±0.7	15
^{116m}In	54.15(16)min	1097.30(20) 1293.54(15)	0.557(15) 0.850(20)	13.5±0.9 17.3±0.5	7 10
^{117m}In	1.940(12)h	cd552.90(20)	0.469(50)	21.4±1.0	15
^{118m}In	4.45(5)min	1050.8(5) c1229.5(5)	0.820(82) 0.96(10)	6.8±1.3 6.2±1.3	1 2
^{116m}Sb	5.000(11)h	1050.8(5) c1229.5(5)	0.82(8) 0.96(10)	7.0±1.5 7.7±0.6	7 8
^{120}Sb	5.760(21)d	c1023.3(4) 1171.7(3)	0.994(3) 1.0	10.8±0.3 10.4±2.0	10 10
^{122}Sb	2.700(10)d	564.24(4)	0.7	14.0±0.5	10
^{124}Sb	60.200(30)d	c602.72(4) c1691.00(4)	0.9792 0.4876(49)	10.1±0.6 10.2±0.6	10 6
^{126}Sb	12.40(10)d	414.80(20) c695.00(20) c697.00(20) c720.50(20) 856.70(20)	0.98 0.997 0.289(70) 0.538(24) 0.176(9)	7.5±0.9 6.84±0.29 12.1±2.2 10.9±0.9 6.5±2.3	2 8 6 4 3
^{127}Sb	3.85(50)d	473.0(4) 685.7(5) 783.7(5)	0.247(9) 0.353 0.145(5)	7.4±1.2 7.2±0.5 7.4±0.9	2 5 2
^{128}Sb	9.010(30)h	c743.30(10) 754.00(10) c813.60(20)	1.00(5) 1.00(5) 0.130(20)	10.6±1.1 1.8±0.5 11±7	9 2 6
^{119m}Te	4.69(5)d	1136.75(7) 1212.73(7)	0.0772(7) 0.667	4.7±1.5 3.72±0.15	1 6
^{121}Te	16.78(35)d	573.139(11)	0.803(17)	5.3±0.5	5
^{131m}Te	1.25(80)	782.49(4) 822.78(4)	0.0778(12) 0.0612(8)	18±4 5.4±1.2	3 1
^{132}Te	3.260(34)d	cd630.22(9) cd667.69(8) d772.60(8)	0.137(6) 0.987(2) 0.762(19)	11.2±0.9 7.1±1.2 6.2±0.3	3 12 7
^{124}I	4.180(21)d	c602.72(4) c1691.02(4)	0.605 0.1041(12)	10.3±0.3 12.8±0.8	10 6
^{126}I	13.02(7)d	388.630(11) c666.330(12)	0.340(7) 0.330(7)	31±10 6.0±1.9	4 6
^{130}I	12.36(1)h	536.090(20) c668.540(10) c739.480(20)	0.99(2) 0.961(25) 0.823(23)	8.1±0.6 11.8±0.6 10.7±3.0	14 4 17

^{131}I	8.04(1)d	364.480(11) 636.793(20)	0.812(16) 0.812(16)	14.2±0.9 13.5±2.7	6. 1
^{132}I	2.2846(4)h	667.70(10)	0.99	8.3±1.2	6
^{133}I	20.80(10)h	529.872(11)	0.863(17)	9.3±0.5	9
^{134}I	52.6(4)	c847.025(25) c884.090(25)	0.954(19) 0.649(9)	2.7±1.2 5.2±0.9	5 7
^{132}Cs	6.48(2)d	c667.5(1)	0.974	6.2±1.8	7
^{136}Cs	13.16(3)d	818.514(12) 1048.070(20) 1235.360(23)	0.997 0.798(30) 0.200(7)	6.01±0.18 7.16±0.24 9.2±0.6	6 6 2
^{140}Ba	12.74(5)d	537.274(20) cd487.029(19) cd815.780(30) cd1596.17(6)	0.2439(21) 0.459(4) 0.2364(17) 0.9540(8)	11.1±2.5+f 4.1±0.5 3.9±0.6 3.4±0.3	1 6 4 11
^{140}La	1.680(18)	c487.029(19) c815.780(30) c1596.17(6)	0.459(4) 0.2364(17) 0.9540(8)	9.3±0.5 6.3±0.6 7.09±0.27	6 4 11
^{135}Ce	17.69(19)h	606.760(20)	0.1881(54)	17.0±2.6	4
^{145}Eu	5.93(5)d	893.738(24)	0.684	1.65±0.20	4
^{146}Eu	4.59(3)d	747.20(12)	0.98	1.16±0.18	3
^{154}Tb	21.4(5)h	c536.25(10) c722.10(20)	0.013 0.058	60±40 13±6	14 17
^{156}Tb	5.35(10)d	534.29(6)	0.67(7)	1.8±0.5	1
^{198}Au	2.700(2)d	411.790(10)	0.955	1.33±0.21	1
^{206}Bi	6.240(3)d	c537.50(5) 803.10(5) c881.01(5)	0.304 0.989 0.662(7)	3.2±0.7+g 1.33±0.21 0.5±0.5	1 1 5
^{240}Am	2.120(13)d	880.80(5) 987.76(6)	0.251(4) 0.731(10)	46.5±1.1 44.7±0.7	10 11

c — complex peak
d — peak corresponding to the decay of daughter nuclei
e — together with 112Ag
f — admixture of 206Bi
g — admixture of 140Ba

Table 3. Formation of nucle in the reactions ^{241}Am(p,xpyn)X. Complex peaks.

№	gen.	E_γ	$T_{1/2}$	Resid.nucl.	Cross-sec.[mb]	Type of cross.-sec.	χ^2
1	1	487.029(19)	12.74d	^{140}Ba	4.1±0.5	C	0.3
	1	487.029(19)	1.68d	^{140}La	9.3±0.5	I	
2	0	536.090(20)	12.36h	^{130}I	8.1±0.6	C	0.3
	0	536.25(10)	21.40h	^{154}Tb	60±40	C	
3	1	552.900(20)	3.36h	^{117m}Cd	6.9±0.7	C	1.0
	0	552.900(20)	1.94h	^{117m}In	21.4±1.0	C	
4	0	554.320(20)	1.47d	^{82}Br	7.55±0.30	I	0.3
	0	554.35(10)	6.47h	^{82m}Rb	12±5	C	
5	1	555.60(10)	9.52h	^{91}Sr	0.9±7.0	C	2.4
	1	555.57(10)	49.71min	^{91m}Y	14±4	I	
6	0	559.10(5)	1.10d	^{76}As	4.5±1.6	C	0.9
	0	559.09(5)	16.19h	^{76}Br	0.6±1.9	C	
7	0	602.72(4)	60.20d	^{124}Sb	10.1±0.6	I	0.9
	0	602.72(4)	4.18d	^{124}I	10.3±0.3	I	
8	1	617.40(20)	21.05h	^{112}Pb	18±0.3	C	1.3
	1	67.40(20)	3.14h	^{112}Ag	20.4±1.7	I	
9	0	919.070(20)	1.47d	^{82}Br	10.5±0.9	I	2.9
	0	619.11(10)	6.47h	^{82m}Rb	6±7	C	
10	1	630.22(9)	3.26d	^{132}Te	11.2±0.9	C	0.6
	1	630.19(2)	2.30h	^{132}I	-	I	
11	1	657.92(10)	16.90h	^{97}Zr	20.7±0.4	C	2.2
	1	657.92(10)	1.20h	^{97}Nb	13.3±0.8	I	
	0	657.77(6)	15.15min	^{89}Rb	4±8	C	
12	0	666.3(2)	12.40d	^{126}Sb	-	I	0.8
	0	666.330(12)	13.02d	^{126}I	6.0±1.9	I	
13	1	667.69	3.26d	^{132}Te	7.1±1.2	C	2.4
	1	667.70(10)	2.28h	^{132}I	8.3±1.2	I	
	0	667.5(1)	6.48d	^{132}Cs	6.2±1.8	I	
14	1s	694.80(20)	21.05h	^{112}Pd	41±9+e	C	0.8
	0	695.00(20)	12.40d	^{126}Sb	6.84±0.29	I	
15	0	698.330(20)	1.47d	^{82}Br	8.5±0.9	I	1.2
	0	698.37(10)	6.47h	^{82m}Rb	2.5±0.8fix	C	
	0	697.00(20)	12.40d	^{126}Sb	12.1±2.2	I	
16	0	719.56(15)	23.35h	^{96}Nb	35±18	I	1.0
	0	720.50(20)	12.40d	^{126}Sb	10.9±0.9	I	
17	0	722.50(10)	51.30min	^{98m}Nb	12.2±0.7	I	1.7
	0	722.10(20)	21.40h	^{154}Tb	13±6	C	
18	0	724.23(4)	63.98d	^{95}Zr	36.0±2.0	C	0.9
	0	724.30(30)	4.44h	^{105}Ru	33.0±1.3	C	
19	0	739.500(15)	2.75d	^{99}Mo	44.1±1.3	C	1.3

	0	739.480(20)	12.36h	^{130}I	10.7±3.0	C	
20	0	744.233(13)	5.59d	^{52}Mn	1.81±0.20	C	1.2
	0	743.36(10)	16.90h	^{97}Zr	19.5±0.8	C	
	0	743.30(10)	9.01h	^{128}Sb	10.6±1.1	C	
21	0	776.490(30)	1.47d	^{82}Br	8.68±0.30	I	1.5
	0	776.52(10)	6.47h	^{82m}Rb	1.4±1.7	C	
22	0	778.22(10)	23.35h	^{96}Nb	13±2	I	2.3
	0	778.22(4)	4.30d	^{96}Tc	2.71±0.29	I	
23	0	812.54(4)	4.30d	^{96}Tc	2.65±0.14	I	
	0	813.60(20)	9.01h	^{128}Sb	11±7	C	
24	1	815.780(30)	12.74d	^{140}Ba	3.9±0.6	C	1.8
	1	815.780(30)	1.68d	^{140}La	6.3±0.6	I	
25	0	827.810(30)	1.47d	^{82}Br	7.3±0.6	I	0.8
	0	827.83(10)	6.47h	^{82m}Rb	7±11	C	
26	0	834.830(21)	312.5d	^{54}Mh	10.1±0.4	I	0.6
	0	834.030(30)	14.10h	^{72}Ga	1.5±0.7	C	
	0	833.990(30)	1.08d	^{72}As	4.2±0.5	C	
27	0	846.750(20)	2.58h	^{56}Mn	6.7±1.6	C	2.0
	0	847.025(25)	52.6 min	^{134}I	2.7±1.2	C	
28	0	849.90(10)	23.35h	^{96}Nb	13.2±1.7	I	1.9
	0	849.86(4)	4.30d	^{96}Tc	2.78±0.19	I	
29	0	881.610(30)	32.77d	^{84}Rd	6.9±0.4	C	2.6
	0	881.01(5)	6.24d	^{206}Bi	0.5±0.5	C	
30	0	884.40(10)	18.4 min	^{104}Tc	14±8	C	1.9
	0	884.090(25)	52.6 min	^{134}I	5.2±0.9	C	
31	0	935.544(12)	5.59d	^{52}Mn	1.9±0.3	C	3.2
	0	934.44(10)	10.15d	^{92m}Nb	0.6±0.4	I	
32	0	983.500(10)	1.82	^{48}Sc	1.35±0.19	I	0.2
	0	983.50(3)	15.97d	^{48}V	3.52±0.17	C	
33	0	1024.30(10)	9.52h	^{91}Sr	15.0±1.8	C	1.7
	0	1023.3(4)	5.76d	^{120}Sb	10.8±0.3	I	
34	0	1043.970(30)	1.47d	^{82}Br	6.5±0.6	I	2.8
	0	1044.08(10)	6.47h	^{82m}Rb	2.5±0.4fix	C	
35	0	1229.5(5)	4.45min	^{118m}In	6.2±1.3	C	
	0	1229.5(5)	5.00h	^{118m}Sb	7.7±0.6	I	
36	0	1312.100(30)	1.82d	^{48}Sc	1.04±0.10	I	0.2
	0	1312.00(3)	15.97d	^{48}V	3.37±0.14	C	
37	0	1317.47(5)	1.47d	^{82}Br	8.0±0.4	I	1.5
	0	1317.43(10)	6.47h	^{82m}Rb	10±12	C	
38	1	1596.17(6)	12.74d	^{140}Ba	3.4±0.3	C	5.2
	1	1596.17(6)	1.68d	^{140}La	7.09±0.27	I	
39	0	1691.00(4)	60.20d	^{124}Sb	10.2±0.6	I	1.1
	0	1691.02(4)	4.18d	^{124}I	12.8±0.8	I	

Table 4. Cross-sections of formation of residual nuclei from the ^{237}Np target

Residual nuclei	Type of decay and cross-sec.	Exper. cross-sec.[mb]	Theor. cross-sec.[mb]	Residual nuclei	Type of decay and cross-sec.	Exper. Cross-sec.[mb]	Theor. cross-sec.[mb]
^{48}Sc	I(β^-)	5.2±1.5	-	^{122}Sb	C(β^-,ε)	18.84±1.7	13.75±0.22
^{48}V	C(β^+)	0.89±0.2	-	^{124}Sb	C(β^-)	16.68±2.0	13.08±0.22
^{56}Mn	C(β^-)	25.35±4.5	0.006±0.006	^{126}Sb	C(β^-)	13.91±2.0	17.74±0.22
^{74}As	I($\beta^\pm$)	3.58±0.5	1.16±0.09	^{127}Sb	C(β^-)	14.74±2.0	22.25±0.22
^{83}Rb	C(ε)	6.13±0.2	14.23±0.1	^{128}Sb	C(β^-)	90.2±1.3	19.66±0.52
^{84}Rb	C($\beta^\pm$)	13.33±0.3	20.25±0.69	^{132}Te	C(β^-)	12.83±3.0	3.2±0.17
^{86}Rb	C(β^-,ε)	17.72±2.0	31.19±0.56	^{133m}Te	C(β^-)	18.44±1.8	0.42±0.006
^{85}Sr	C(ε)	9.6±2.0	14.28±0.18	^{124}I	I(β^+,ε)	17.29±2.0	19.65±0.31
^{91}Sr	C(β^-)	29.11±3.0	25.02±0.4	^{131}I	C(β^-)	20.36±1.9	30.55±0.49
^{87}Y	C(β^+,ε)	6.65±0.1	7.04±0.28	^{134}I	C(β^-)	12.86±1.5	2.04±0.14
^{88}Y	C(β^+,ε)	10.44±0.9	17.7±0.15	^{136}Cs	I(β^-)	9.14±0.4	3.57±0.15
^{89}Zr	C(β^+,ε)	4.62±0.5	6.83±0.19	^{138}Cs	C(β^-)	14.93±1.4	0.49±0.03
^{95}Zr	C(β^-)	59.24±6.0	40.27±0.07	^{131}Ba	C(β^+,ε)	71.09±13	16.82±0.22
^{95}Nb	C(β^-)	22.31±2.0	49.25±0.13	^{140}Ba	C(β^-)	22.92±2.0	0.28±0.03
^{99}Mo	C(β^-)	73.13±6.0	36.33±0.2	^{145}Eu	C(β^+,ε)	0.83±0.01	0.025±0.01
^{95m}Tc	C(β^+,ε)	2.32±0.15	0.63±0.03	^{146}Eu	I(β^+,ε)	4.2±0.2	0.006±0.006
^{96}Tc	C(β^+,ε)	5.65±0.9	1.73±0.13	^{147}Eu	C(β^+,ε)	1.93±0.3	0.006±0.006
^{103}Ru	C(β^-)	62.91±1.0	22.39±0.16	^{146}Gd	C(β^+,ε)	1.39±0.02	-
^{105}Ru	C(β^-)	19.63±2.0	12.32±0.013	^{152}Tb	C(β^+,ε)	26.77±3.0	-
^{106m}Rh	I(β^-)	55.32±3.0	2.09±0.05	^{171}Lu	C(β^+)	2.41	-
^{106m}Ag	I($\beta^\pm$)	6.18±0.8	0.82±0.036	^{185}Os	C(ε)	2.76±0.1	-
^{110m}Ag	I(β^-,ε)	17.97±2.0	2.05±0.1	^{188}Pt	C(ε)	0.46±0.08	-
^{115g}Cd	C(β^-)	64.61±6.0	3.14±0.16	^{206}Po	C(ε)	3.78±0.7	2.65±0.1
^{117m}Cd	C(β^-)	17.44±4.0	1.27±0.11	^{230}Pa	I(ε)	1.6±0.15	23.54±0.19
^{125}Sn	C(β^-)	6.59±0.4	7.47±0.22	^{234}Np	C(β^+,ε)	2.21±0.4	75.0±1.16
^{118m}Sb	I(β^+,ε)	10.36±1.3	9.04±0.14	^{238}Np	C(β^-)	15.77±1.4	-
^{120}Sb	I(β^+,ε)	14.71±1.6	13.68±0.04				

Table 5. Cross-sections of formation of residual nuclei from the ^{241}Am target

Residual nuclei	Type of decay and cross-sec	Exper. Cross-sec.[mb]	Theor. cross-sec.[mb]	Residual Nuclei	Type of decay and cross-sec	Exper. Cross-sec.[mb]	Theor. cross-sec.[mb]
^{48}Sc	I(β^-)	1.11±0.09	-	^{108}Rh	I(β^-)	11.6±1.5	6.03±0.18
^{48}V	C(β^+)	3.44±0.11	-	^{112}Pd	C(β^-)	21±0.7	4.76±0.20
^{52}V	C(β^-)	2.3±0.6	-	^{106m}Ag	I(β^+,β^-)	2.5±0.3	1.57±0.05
^{52}Mn	C(β^+,ε)	1.74±0.11	-	^{110m}Ag	I(β^-,ε)	11.6±2.4	3.86±0.12
^{54}Mn	I(ε)	10.1±0.4	-	^{112}Ag	I(β^-)	20.4±1.6	3.40 ±0.26
^{56}Mn	C(β^-)	6.7±1.6	-	^{115}Cd	C(β^-)	19.2±0.9	6.70±0.30
^{72}Ga	C(β^-)	1.5±0.7	0.38±0.09	^{117m}Cd	C(β^-)	6.9±0.7	2.66±0.05
^{72}As	C(β^+,ε)	4.2±0.5	0.022	^{116m}In	I(β^-)	16.4±0.8	5.44±0.13
^{76}As	I(β^-)	4.5±1.6	1.45±0.06	^{117m}In	C(β^-)	21.4±1.0	9.87±0.35
^{76}Br	C(β^+)	0.6±1.8	0.02±0.01	^{118m}In	I(β^-)	6.5±0.9	4.71±0.21
^{82}Br	I(β^-)	8.0±0.3	4.79±0.13	^{118m}Sb	I(β^+,ε)	7.6±0.6	8.72±0.09
^{84}Br	C(β^-)	9.2±1.4	1.16±0.07	^{120}Sb	I(β^+,ε)	10.8±0.3	12.9±0.6
^{84m}Br	I(β^-)	2.7±0.6	-	^{122}Sb	C(β^-,ε)	14.0±0.5	13.2±0.1
^{82m}Rb	C(β^+,ε)	2.1±1.0	1.84±0.08	^{124}Sb	C(β^-)	10.2±0.4	13.4±0.2
^{84}Rb	C(β^+,β^-)	6.9±0.4	13.1±0.2	^{126}Sb	C(β^-)	7.3±0.7	9.56±0.23
^{86}Rb	C(β^-)	2.02±0.29	13.6±0.1	^{127}Sb	C(β^-)	7.3±0.5	9.07±0.19
^{89}Rb	C(β^-)	11.1±1.5	1.98±0.13	^{128}Sb	C(β^-)	3.3±1.0	3.51±0.08
^{91}Sr	C(β^-)	15.0±1.7	5.61±0.20	^{119m}Te	I(β^+,ε)	3.73±0.15	11.2±0.30
^{92}Sr	C(β^-)	11.8±0.5	3.03±0.07	^{121}Te	C(β^+,ε)	5.3±0.5	29.3±0.4
^{93}Sr	C(β^-)	10.4±2.2	1.09±0.10	^{131m}Te	I(β^-)	6.5±1.1	3.18±0.13
^{84m}Y	I(β^+,ε)	3.1±0.9	-	^{132}Te	C(β^-)	6.7±0.5	1.30±0.08
^{87}Y	C(β^+,ε)	4.40±0.27	9.22±0.22	^{124}I	I(β^+,ε)	10.6±0.8	17.6±0.2
^{88}Y	C(β^+,ε)	6.2±0.4	20.5±2.4	^{126}I	I(β^+,β^-)	6.8±1.8	20.6±0.5
^{91m}Y	C(β^-)	14±4	28.9±5.0	^{130}I	i(β^-)	10.0±0.9	16.5±0.5
^{95}Y	C(β^-)	17.4±3.6	3.69±0.22	^{131}I	C(β^-)	14.1±0.9	20.2±0.5
^{89}Zr	C(β^+,ε)	3.79±0.27	11.0±0.4	^{132}I	I(β^-)	8.3±1.2	9.03±0.14
^{95}Zr	C(β^-)	36.3±1.7	18.3±0.4	^{133}I	C(β^-)	9.3±0.5	6.18±0.14
^{97}Zr	C(β^-)	20.4±0.4	7.22±0.32	^{134}I	C(β^-)	4.3±0.7	0.980±0.065
^{92m}Nb	I(β^+,ε)	0.6±0.4	9.42±0.37	^{132}Cs	I(β^+,β^-)	6.2±1.7	12.2±0.4
^{95}Nb	C(β^-)	16.8±2.0	41.8±0.5	^{136}Cs	C(β^-)	6.6±0.5	2.05±0.04
^{96}Nb	I(β^-)	13.6±0.3	18.8±0.4	^{140}Ba	C(β^-)	3.64±0.24	0.045±0.03
^{97}Nb	C(β^-)	13.3±0.8	24.4±0.5	^{140}La	I(β^-)	7.4±0.5	0.113±0.03
^{98m}Nb	I(β^-)	13.9±0.5	21.8±0.4	^{135}Ce	C(β^+,ε)	17.0±2.5	3.75±0.05
^{99}Mo	C(β^-)	44.1±1.3	42.2±0.5	^{145}Eu	C(β^+,ε)	1.65±0.19	0.045±0.020
^{96}Tc	C(β^+,ε)	2.71±0.28	3.40±0.10	^{146}Eu	C(β^+,ε)	1.16±0.17	0.022±0.014
^{104}Tc	C(β^-)	22±6	23.9±0.3	^{154}Tb	C(β^+,ε)	13±6	-
^{103}Ru	C(β^-)	62.9±3.4	43.7±0.5	^{156}Tb	C(ε)	1.7±0.5	-
^{105}Ru	C(β^-)	33.8±1.2	29.0±0.7	^{198}Au	C(β^-)	1.33±0.20	-
^{105}Rh	C(β^-)	77±13	36.8±0.7	^{206}Bi	C(ε)	1.21±0.25	1.19±0.20
^{106m}Rh	I(β^-)	15.0±2.3	27.9±0.3	^{240}Am	I(ε)	45.3±0.8	-

REFERENCES

[1] *Kusters H.* Atomwirtschaft, 1990, v.35, 6, 287.

[2] *W.Gudowski* Nucl. Phys. A654 (1999) 436-457.

[3] *Yu.P.Sivintchev* Atomic technique out of boundary 1992, v.2, p.1, v.11, p.3.

[4] *A.S.Nikiforov.* Atomic energy 1991, 70, p.188.

[5] M.I.Krivopustov et al. JINR Preprint E1-97-59 (1997), Journal of Radioanalytical and Nuclear Chemistry 222, (1997) 267.

M.Ochs et al. Preprint of JINR E1-99-1. Submitted to NIM.

[6] *V.F.Batiaev* PhD Thezis JINR, Dubna, 1999.

[7] *Yu. E.Titarenko et al.* Nuclear Instruments and Methods in Physics Research A 414 (1998) 73.

[8] *T. Nishida, Y. Nakahara* Kerntechnik 50 (1987) 3.

[9] *L.Moens et al.* Nuclear Instruments and Methods 187(1981), 451..

[10] *J.B.Cumming* Ann. Rev.Nucl.Sci. 13 (1963) 261

[11] *R.Michel et al.* Nuclear Instruments and Methods in Physics Research B 103 (1995) 185.

[12] *Yu.V.Aleksandrov et al.* Abstracts of XLVI Meeting on Nuclear Spectroscopy and Nuclear Structure, *Moscow, 1996, 221.*

[13] *J.Frana* Acta Polytechnica-Nukleonika, 1998, v.38, p.127.

[14] *N.Reus, W.Westmeier* Atomic Data and Nuclear Tables, 29(1983), 1-192

[15] *J.Adam et al.* Preprint JINR P10-2000-28.

[16] *K.Michel, P.Nagel* International Codes and Model Intercomparison for Intermediate Energy Activ. Yields. NEA/OECD, Paris 1997, NSC/DOC(97)-1.

[17] *H.R.Heydegger, A.L.Turkevich, A.Van Ginneken, P.N.Walpole* Phys.Rev. 1976, C14, 1506.

[18] *S.S.Lomakin, V.N.Petrov, P.S.Samoilov* Radiometria of neutrons by activation methods. Moscow, 1983.

[19] *A.Polanski, A.N.Sosnin, V.D.Toneev* JINR Preprint E2-91-562, Dubna, 1991.

F.G. Zheregy, J.J.Musulmanbekov Program for calculation of intranuclear cascade in nuclear-nucleus interaction. Dubna, JINR B3-10-84-873, 1984r.

[20] *V.S.Barashenkov, V.D.Toneev,* Interaction of hight energy particles and atomic nuclei with nuclei. Moscow , 1972, p.568.

[21] *V.E.Aleqsandryan et al.* Physics of Atomic Nuclei 59 (1996) 592.

Received by Publishing Department
on October 26, 2000.

Адам И. и др.
E15-2000-256

Исследование образования остаточных ядер
из радиоактивных мишеней ^{237}Np и ^{241}Am
в реакциях с протонами при энергии 660 МэВ

Радиоактивные мишени ^{237}Np и ^{241}Am облучались протонным пучком с энергией 660 МэВ. Определены сечения образования 80 и 60 остаточных ядер из ^{241}Am и ^{237}Np соответственно. Экспериментальные результаты сравниваются с расчетными, сделанными по каскадно-испарительной модели.

Работа выполнена в Лаборатории ядерных проблем им. В.П.Джелепова ОИЯИ.

Препринт Объединенного института ядерных исследований. Дубна, 2000

Adam J. et al.
E15-2000-256

Investigation of the Formation of Residual Nuclei
from the Radioactive ^{237}Np and ^{241}Am Targets
in the Reaction with 660 MeV Protons

Radioactive ^{237}Np and ^{241}Am targets were irradiated by proton beams with energy 660 MeV. The cross-sections of formation of 80 and 60 residual nuclei from ^{241}Am and ^{237}Np are determined. The experimental results are compared with the theoretical cross-sections calculated by the cascade-evaporation model.

The investigation has been performed at the Dzhelepov Laboratory of Nuclear Problems, JINR.

Preprint of the Joint Institute for Nuclear Research. Dubna, 2000

Макет Т.Е.Попеко

Подписано в печать 21.11.2000
Формат 60 × 90/16. Офсетная печать. Уч.-изд. листов 1,9
Тираж 300. Заказ 52359. Цена 2 р. 30 к.

Издательский отдел Объединенного института ядерных исследований
Дубна Московской области